

Analysis of reinforced concrete walls due to impact of vehicles during tornadoes

Manoj Madurapperuma*, Kazukuni Niwa*, Zhelin Zhao**

*Terrabyte(Japan) Co.,Ltd (〒113-0034 3F.,NOV bldg,yushima 3-10-7, Bunkyo, Tokyo)

**Terrabyte(Shanghai) Co.,Ltd (〒200-001 Room E-F,21F.,No.1 Plaza,800 Nanjing Road East,Huangpu District,Shanghai)

Abstract

Protection of critical facilities against impact of heavy objects during tornadoes has drawn much attention after the recent destructive tornadoes. Damage to reinforced concrete structures due to impact of a heavy vehicle during tornadoes is becoming an important consideration particularly for critical facilities. In the present study, impact damage to reinforced concrete walls is evaluated using two types of detailed finite element models of vehicles having different weights and sizes, and reinforced concrete walls. It is seen that damage to the impacted wall varies depending on vehicle type, speed and impact orientation. Set of equations are proposed to approximately estimate peak impact force on walls due to impact of vehicles during tornadoes. Further, vehicle velocity limits for scabbing damage and perforation damage to impacted walls are also presented. The results could be useful for engineers and researchers.

Introduction

Damage to buildings and infrastructure due to wind-borne heavy objects has drawn much attention after destructive tornadoes in the past. Protection of critical structures against an accidental impact of a vehicle during tornadoes is becoming an important consideration particularly for critical facilities. In the present study, impact performance of reinforced concrete walls is evaluated using detailed finite element models of a vehicle and reinforced concrete wall. Two types of vehicles and two RC wall configurations have been considered. Different impact orientations are also considered to study severe impact scenarios. The study provides detailed information on the impact performance of reinforced concrete walls which will be useful for engineers and researchers.

Finite Element Modeling of Vehicle Impact on Walls

To simulate impact between the vehicle and RC wall, LS-DYNA [1] is used and the finite element models incorporate inelastic material models with strain rate effects, material erosion to capture the failure process of damaged components in the vehicle and wall, and dynamic interaction between various parts of the vehicle and wall using appropriate contact algorithms. All simulations are carried out using an explicit solver where the time step is determined internally based on the smallest element size in the model and updated in each analysis step. The developed RC wall model is validated using experimental impact test results of RC walls. The vehicle models and wall configurations used in the analysis are discussed below.

(1) Vehicle Models

Vehicle models created by the National Crash Analysis Center (NCAC) with George Washington University [2] were chosen for the present study. The models have been created using detailed vehicle geometry data and component level material tests, and have been validated for vehicle impact analysis by NCAC.

Figure 1 shows vehicle models used in the present study. The models used in the present study are the Taurus (Fig. 1a) and Wagon (Fig. 1b). The Taurus model consists of 26,793 nodes and 28,363 elements arranged in 133 parts with different material models. The total mass of the model is 2 ton. The Wagon model consists of 295,447 nodes and 294,483 elements arranged in 400 parts with different material models. The total mass of the model is 3 ton. Nonlinear material models have been used in the most important parts of the vehicles such as bumper, rails, and frames.



Fig.1 FE vehicle models used in the analysis (dimensions are in mm)

(2) Wall Model

Two types of walls are considered and have the same size of 5 m x 5 m. The thicknesses of walls are 150 mm and 450mm. The compressive strength of concrete is 22 MPa (the same value used in validation study) and the reinforcement ratio is 0.8% by volume each way in all three

walls. Details of rebar sizes are #4(12.7 mm) for 150 mm wall, #5(15.9 mm) for 250 mm wall, and #6(19.1 mm) for 450 mm wall. The yield strength of rebar is 345 MPa, tensile strength is 490 MPa and failure strain is 18%. These material data are the same as material data used in the model validation study discussed in the following section.

Figure 2 shows wall size and reinforcement arrangement. Solid elements and beam elements are used to model concrete and reinforcement, respectively. Perfect bond between concrete solid elements and reinforcement beam elements is considered. The constraints provided by beams and columns at the periphery are included in the model by constraining nodes on the surface of four-sides.

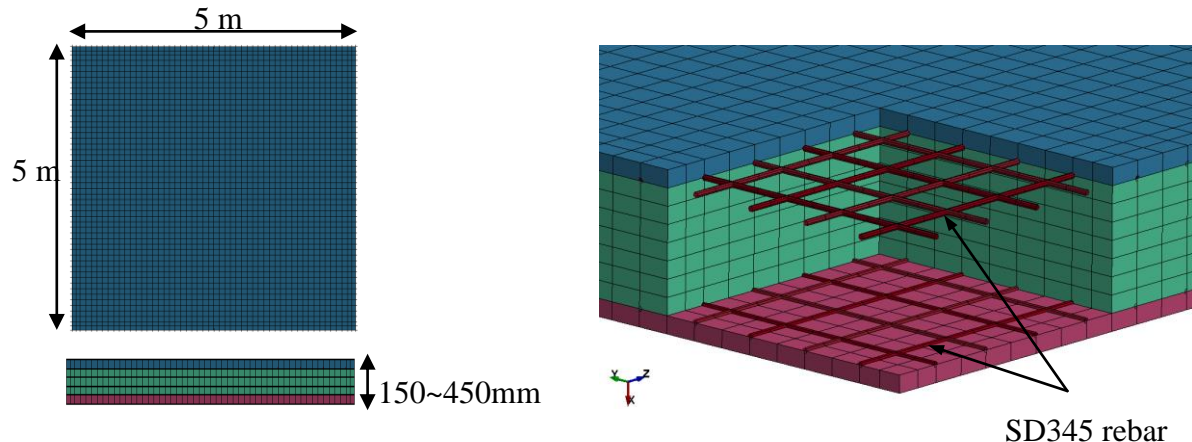


Fig.2 Details of the wall configuration

The material model MAT_072R3 (KCC model) is chosen as the constitutive model for concrete [3,4]. This KCC material model has been extensively used for investigation of RC structural response to impact loads, and it is robust and has performed well in simulating experimentally observed behavior. It is a three-invariant model that includes strain rate effect and damage. The model provides user control of damage parameters for robust and accurate simulation of damage to concrete structures. The selection of appropriate parameters for the KCC model is carried out by using experimental results of impact tests on RC walls as described in model validation. The KCC model does not allow material erosion through removal of highly distorted elements from the model. Hence, complete removal of these distorted elements is considered using MAT_ADD_EROSION option which provides a way of automatically removal of elements from the calculation when the specified erosion criterion is satisfied. It is found from validation study and preliminary analysis of vehicle-wall impact that the appropriate values for maximum principal strain and shear strain are 0.1 and 0.1, respectively [4]. The material model MAT_024 is used to model reinforcement.

Contact between the vehicle and wall is defined using a contact algorithm which has the capability to simulate eroding contacts, and self-contact among the vehicle components.

Validation of RC Wall Model

(1) Description of the Experiment

Full-scale impact tests have been carried out to investigate local damage to RC walls by the impact of aircraft engine [5,6]. Experimental results from two types of wall configurations

namely, test L1 and L5 are used for the validation study. In the test L1 wall indicated just perforation mode of damage where as in the test L5 the wall indicated penetration damage. The test L1 wall has the dimension of 7 m x 7 m x 0.9 m. The test L5 wall has the dimension of 7 m x 7 m x 1.6. The walls have unconfined compressive strength of concrete 22 MPa, and reinforcement ratio of 0.8%. In the both tests walls were vertical and restrained at their four corners. The full-scale engine model was a cylindrical shape with three circular plates at both ends and one at mid region. The engine model was 0.76 m in diameter, 2.378 m in length and has 1911 kg and 1616 kg in mass for L1 and L5, respectively. It was allowed to impact at the center region of each wall at an impact velocity of 205 m/s and 214 m/s for tests L1 and L5, respectively.

(2) Finite Element Model and Comparison of Results

As shown in Fig. 3, detailed one-quarter model is developed following the modeling procedure adopted for RC wall, as discussed in the above section. Damage parameters in the KCC model is chosen to simulate experimentally observed damage behavior of the wall.

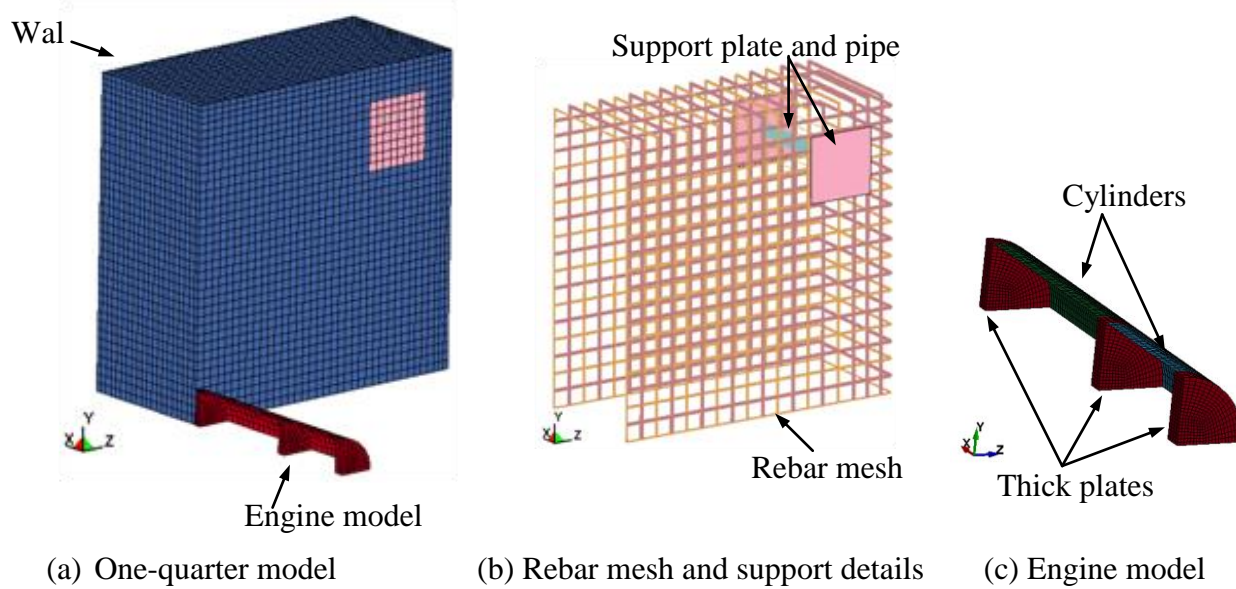


Fig. 3 One-quarter finite element model of engine impact on RC wall

Figure 4 shows comparison of experiment and analysis results of walls front and back faces after the impact of the engine model. Here the full model is replicated from the one-quarter model for clarity. As shown in figure 4 for test L1, the wall indicates just perforation mode of damage where the engine model stops due to reinforced cage although concrete is completely damage in the mid region. The total reaction force is calculated using results of one-quarter models and multiplying by four to compare with experimental results. The reaction force time-history obtained using the analysis is in good agreement with the experiment results particularly initial increase in force and peak force. Displacement time histories of the wall were not available due to severe damage to the wall in test L1.

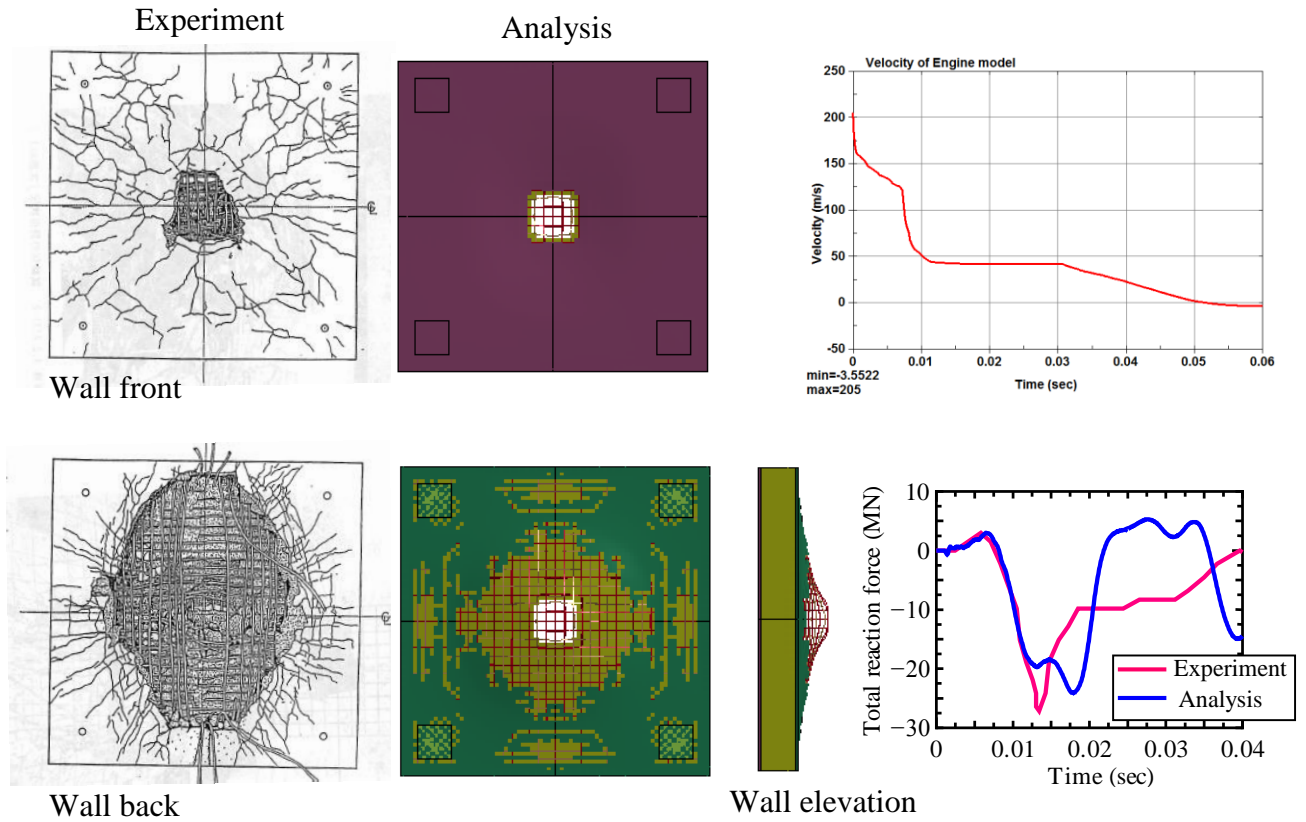


Fig. 4 Comparison of experimental and analysis results for test L1

Figure 5 shows experimental and analysis results of test L5. Here also the full model is replicated from the one-quarter model for clarity. It has been reported that the depth of penetration was 210 mm and only cracks could be seen at the back of the wall in the experiment. In the analysis the depth of penetration of the wall is 270 mm. The figure compares displacement and total reaction force obtained in the simulation with the experimental results. The total reaction force is calculated using results of one-quarter model and multiplying by four to compare with experimental results. The displacement is measured at the center point back of the wall and the reaction forces are calculated at the restrained points. As shown in Fig. 5, analysis results show that displacement does not continuously increase due to failure of the front part of the engine which reduces impact load on the wall. The total reaction force does not continuously increase because of failure of the engine. Both peak displacement and peak reaction force are nearly the same as that of experiment. Based on these validation results, it is seen that the calibrated model has the capability of simulating the perforation as well as penetration damage behavior of the wall similar to damage behavior reported in the experiment.

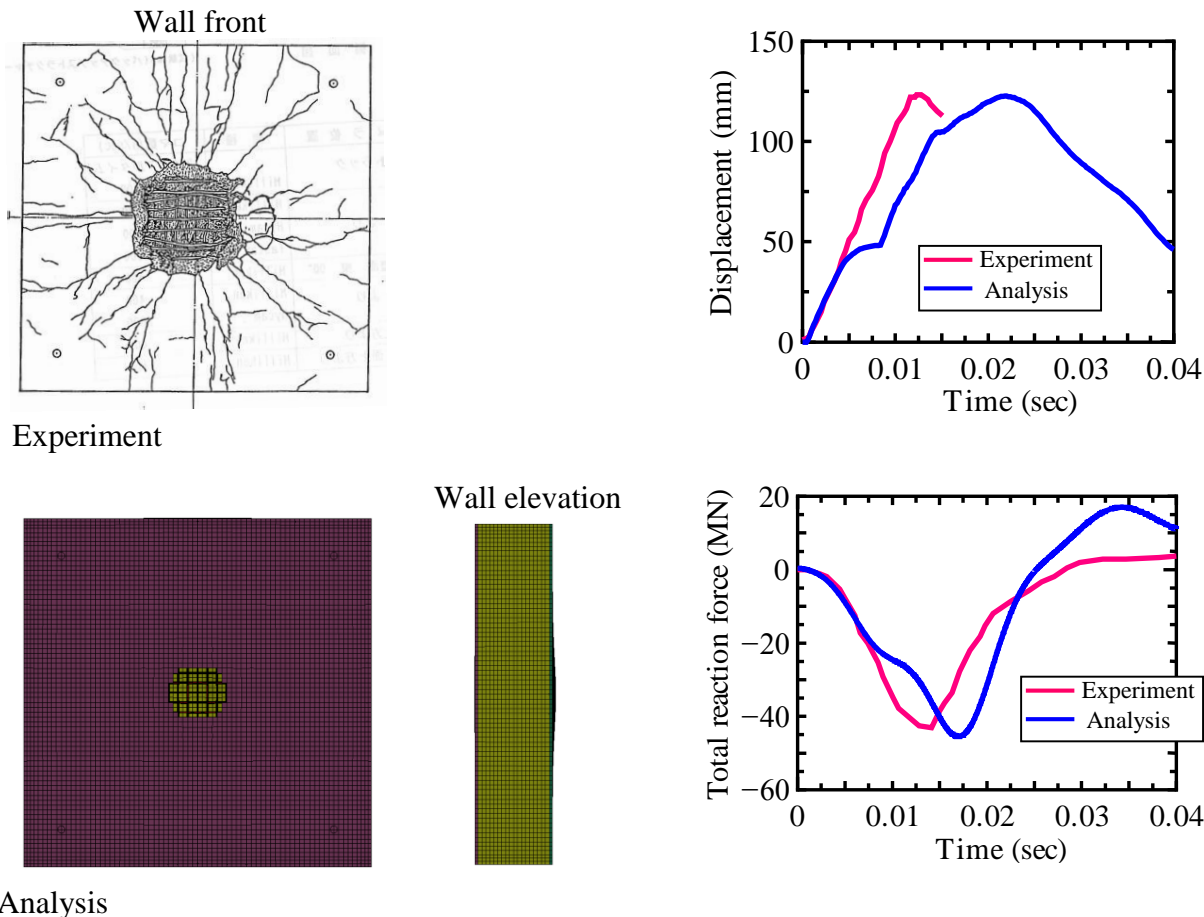


Fig. 5 Comparison of experimental and analysis results for test L5

Vehicle Wall Impact Analysis and Results

(1) Analysis Procedure

The impact velocity of the vehicle is varied with a minimum of 10 m/s to maximum of 60 m/s. As shown in Fig. 6, two vehicle-wall impact configurations for each vehicle namely, front impact and side impact are considered in the analysis.

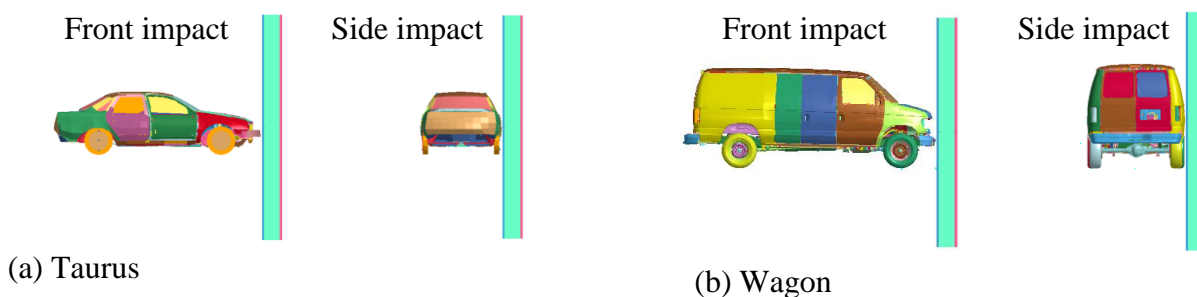


Fig. 6 Vehicle-wall impact configurations

(2) Peak Impact Force on a Rigid Wall

Impact of vehicles on a rigid wall using impact configurations discussed above are considered to study behavior of impact force-time history. Figure 7 shows mass distribution of vehicle models and impact force-time history for the impact velocity of 50 m/s. In both vehicle models front is heavier than rear due to vehicle engine and this heaviest mass is located within a 1 m from the front of the vehicle models. It is also seen that the rear wheel system is relatively heavy in the case of Wagon model compared to Taurus model. Due to mass conservation at the front of the vehicle models, in the case of front impact the peak impact force can be seen at the early stage of contact for both vehicles. It is seen that peak impact force is higher and occurs early in side impact compared to front impact for both vehicles. In the case of side impact contact area between the vehicle and wall increases and stiff members in door frames as well as chassis directly come into contact with the wall at early stage and therefore impact force is high. On the other hand in the case of front impact, vehicle buffer systems come into contact first and stiff engine parts of the vehicle come into contact at a later stage and therefore, peak impact force occurs later in front impact configurations.

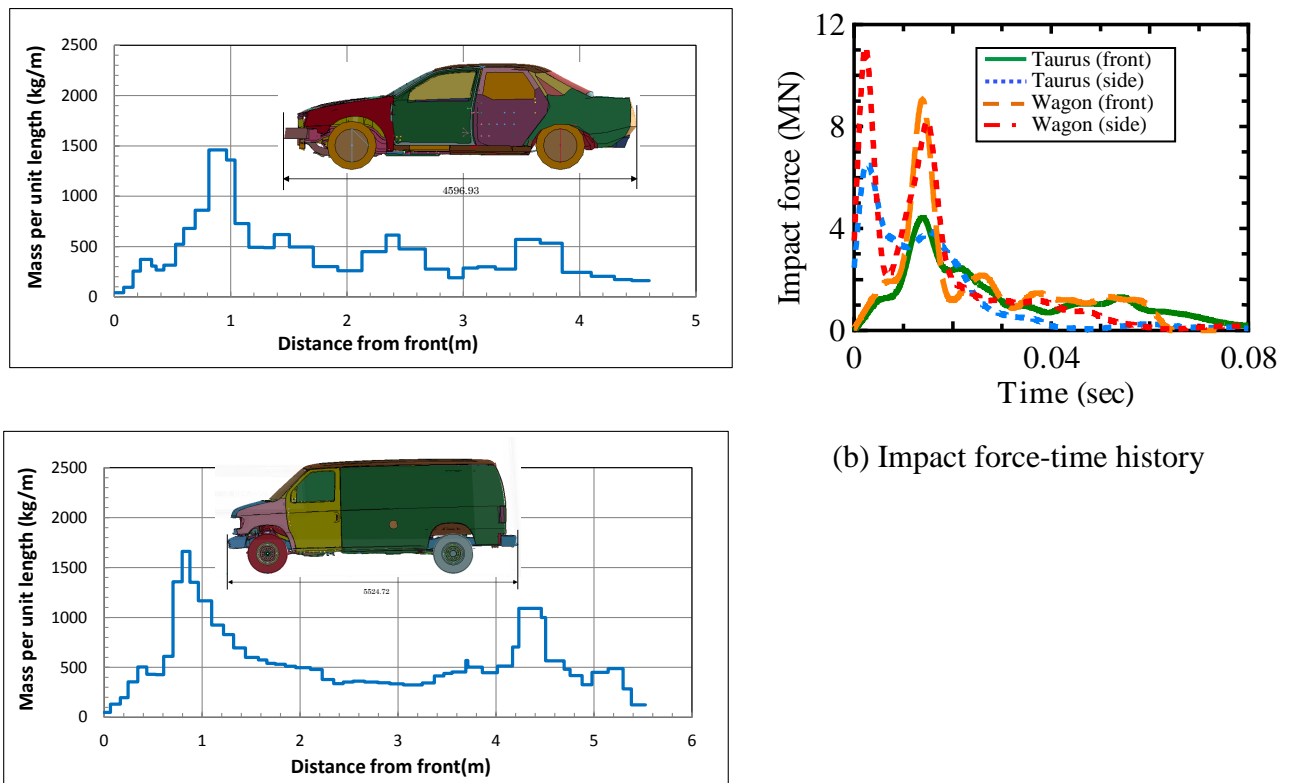


Fig. 7 Mass distribution of vehicle models and impact force-time history for different vehicle-wall impact configurations

(3) Damage Behavior of RC Walls

Figure 8 shows damage evolution of the 150 mm wall due to front and side impact of Taurus vehicle for impact velocity of 50 m/s. The damage to the wall is severe where most of the concrete at the vicinity of the contact region in the front and back has removed. Vehicle does not perforate and is retained by the reinforcement with the support of remaining concrete.

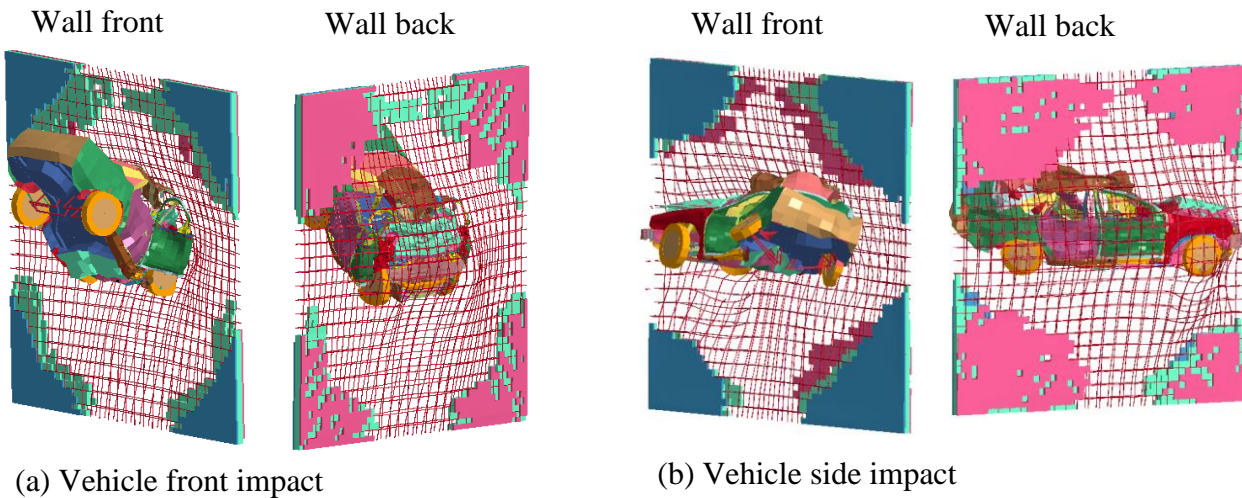


Fig. 8 Evolution of damage to the 150 mm wall due to front and side impact of Taurus vehicle for impact velocity of 50 m/s

Figure 9 shows damage pattern of the 150 mm wall due to front and side impact of Taurus vehicle for impact velocity of 50 m/s. As shown in Fig. 9(b) for side impact, the left side of the wall suffers more damage compared to the right side. In the Taurus vehicle model the engine is located close to left side, and therefore, stiff parts directly come into contact with the wall causing more damage to left side.

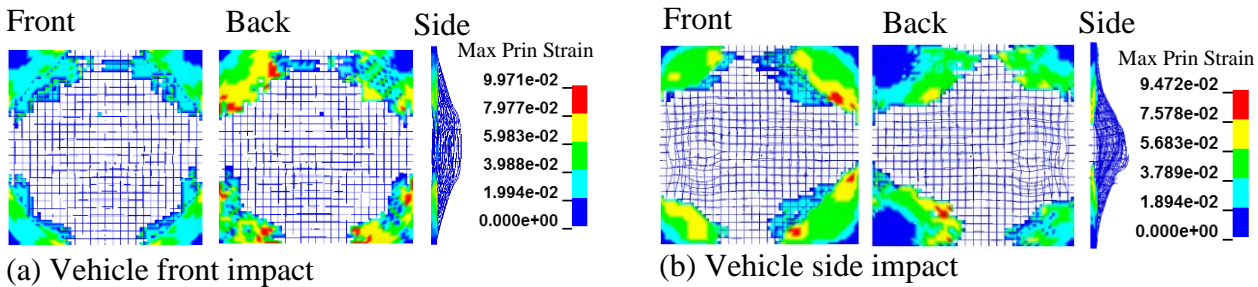


Fig. 9 Damage pattern of the 150 mm wall due to front and side impact of Taurus vehicle for impact velocity of 50 m/s

Figure 10 shows damage evolution of the 450 mm wall due to front and side impact of Taurus vehicle for impact velocity of 50 m/s. The damage to the wall is less where only spalling of concrete at the back is seen. Most of the energy is absorbed by the vehicle due to its inelastic deformations.

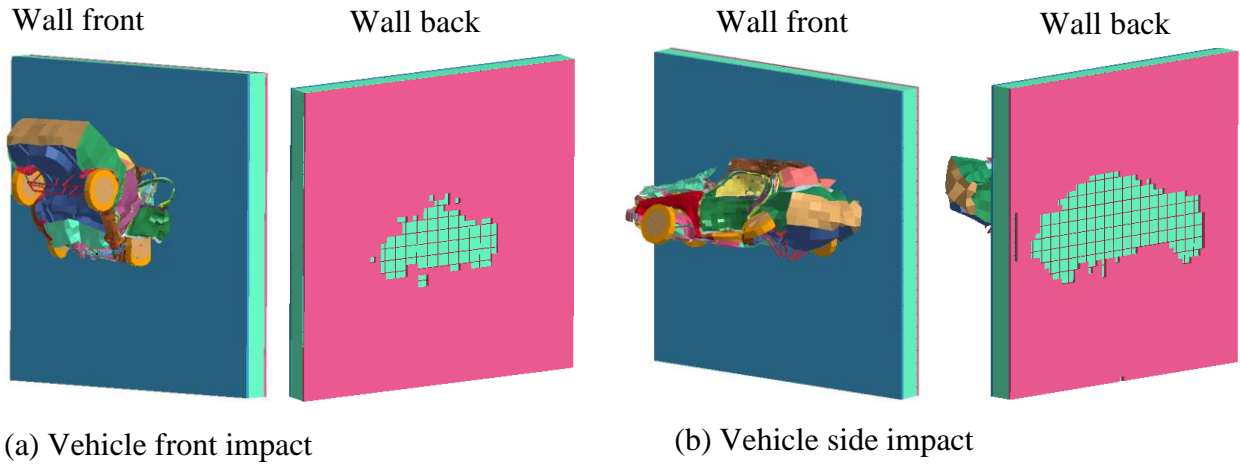


Fig. 10 Evolution of damage to the 450 mm wall due to front and side impact of Taurus vehicle for impact velocity of 50 m/s

Figure 11 shows damage pattern of the 450 mm wall due to front and side impact of Taurus vehicle for impact velocity of 50 m/s. As shown in Fig. 11(b) for side impact, the left side of the wall suffers more damage compared to the right side because in the Taurus vehicle model the engine is located close to left side.

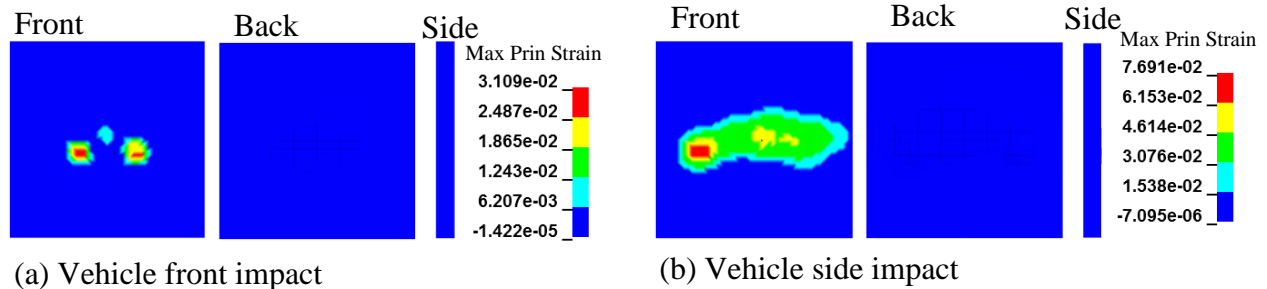


Fig. 11 Damage pattern of the 450 mm wall due to front and side impact of Taurus vehicle for impact velocity of 50 m/s

In the case of Wagon vehicle for impact velocity of 50 m/s, the damage to the 150 mm wall is very severe where vehicle has nearly perforated through the wall in both impact configurations, and these results are not shown in this paper.

Figure 12 shows damage evolution of the 450 mm wall due to front and side impact of Wagon vehicle for impact velocity of 50 m/s. The damage to the wall is less where only spalling of concrete at the back is seen. Most of the energy is absorbed by the vehicle due to inelastic deformations

Figure 13 shows damage pattern of the 450 mm wall due to front and side impact of Wagon vehicle for impact velocity of 50 m/s.

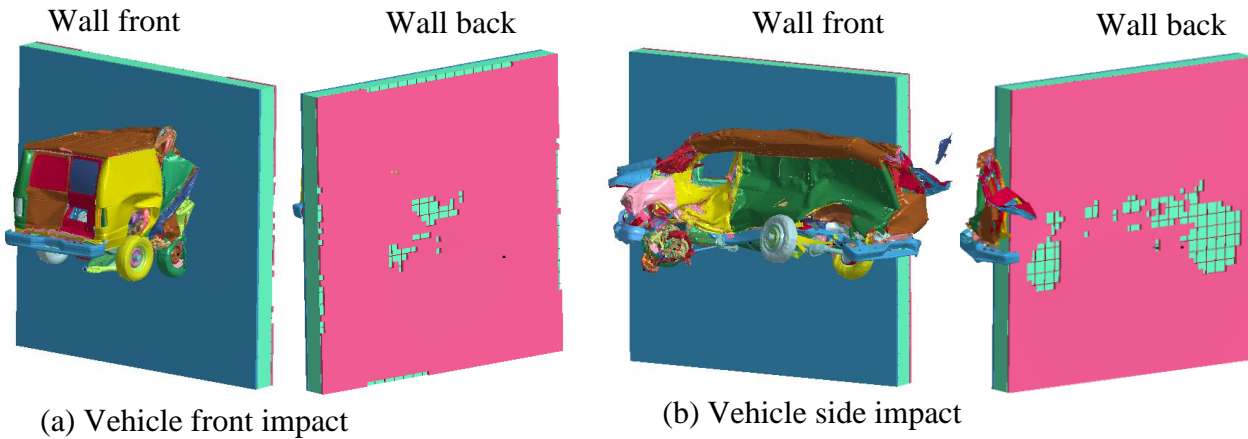


Fig. 12 Evolution of damage to the 450 mm wall due to front and side impact of Wagon vehicle for impact velocity of 50 m/s

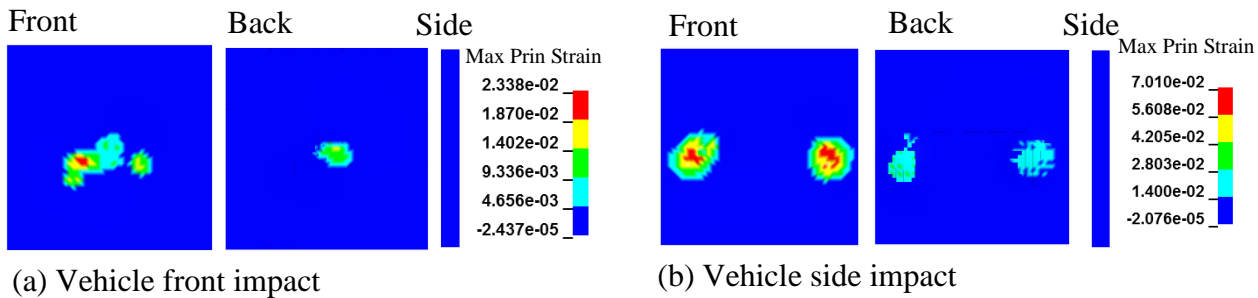
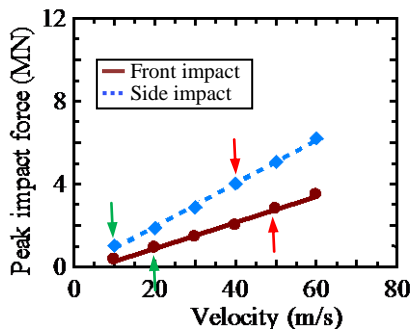


Fig. 13 Damage pattern of the 450 mm wall due to front and side impact of Wagon vehicle for impact velocity of 50 m/s

(4) Equations for Peak Impact Force on RC Walls

Peak impact force obtained for the Taurus vehicle impact on 150 mm wall for front and side impact configurations is shown in Fig. 14. The arrows in the figure indicate velocity limits for scabbing and perforation damage to the wall for each impact configurations.



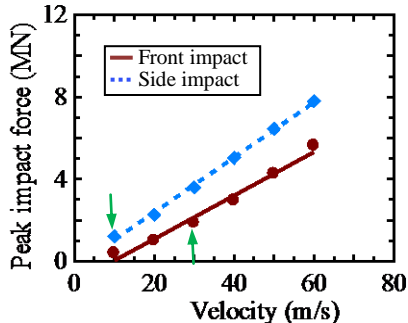
Average peak impact force is given by following equations:

$$F_{peak, front impact} = 0.0624v - 0.3533$$

$$F_{peak, side impact} = 0.1043v - 0.1387$$

Fig. 14 Peak impact force obtained for the Taurus vehicle impact on 150 mm wall for front and side impact configurations, green arrow indicates velocity limit for scabbing damage, red arrow indicates velocity limit for perforation damage

Peak impact force obtained for the Taurus vehicle impact on 450 mm wall for front and side impact configurations is shown in Fig. 15. The arrows in the figure indicate velocity limits for scabbing damage to walls.



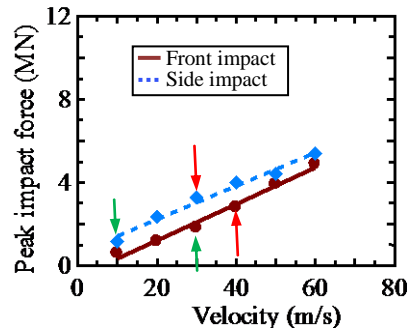
Average peak impact force is given by following equations:

$$F_{peak, front impact} = 0.1056v - 1.0153$$

$$F_{peak, side impact} = 0.1338v - 0.288$$

Fig. 15 Peak impact force obtained for the Taurus vehicle impact on 450 mm wall for front and side impact configurations, arrow indicates velocity limit for scabbing damage

Peak impact force obtained for the Wagon vehicle impact on 150 mm wall for front and side impact configurations is shown in Fig. 16. The arrows in the figure indicate velocity limits for scabbing and perforation damage to the wall for each impact configurations.



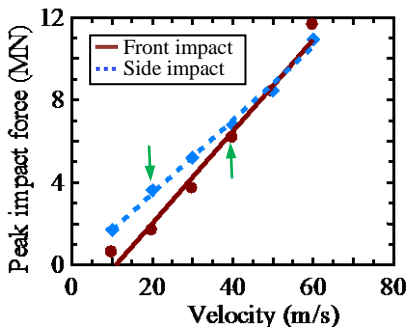
Average peak impact force is given by following equations:

$$F_{peak, front impact} = 0.0874v - 0.53$$

$$F_{peak, side impact} = 0.0803v + 0.626$$

Fig. 16 Peak impact force obtained for the Wagon vehicle impact on 150 mm wall for front and side impact configurations, arrow indicates perforation limit, green arrow indicates velocity limit for scabbing damage, red arrow indicates velocity limit for perforation damage

Peak impact force obtained for the Wagon vehicle impact on 450 mm wall for front and side impact configurations is shown in Fig. 17. The arrows in the figure indicate velocity limits for scabbing damage to walls.



Average peak impact force is given by following equations:

$$F_{peak, front\ impact} = 0.2221v - 2.4133$$

$$F_{peak, side\ impact} = 0.1778v - 0.0987$$

Fig. 17 Peak impact force obtained for the Wagon vehicle impact on 450 mm wall for front and side impact configurations, arrow indicates velocity limit for scabbing damage

Conclusions

It is seen that the KCC concrete model can be used to simulate penetration as well as perforation damage to RC walls. Further, the model is very robust and it provides user control of damage parameters for accurate simulation of damage to concrete structures.

For the vehicle considered, it is seen that side impact of the vehicle is more critical than front impact for the both types of walls. Most of energy dissipaters are designed for front impact of the vehicle and therefore, most of kinetic energy of the vehicle dissipated through plastic deformation of the vehicle when the vehicle front side impacts on the walls. The side of the vehicle does not have such energy absorbers so that greater amount of kinetic energy can transfer to walls causing severe damage in the case of side impact. Further, the contact area is large in the case of side impact compared to front impact of the vehicle resulting large contact forces between vehicle and the wall which cause greater damage to the wall. It is seen that the increase of wall thickness considerably reduce damage to the wall. The proposed equations for peak impact force could be useful for engineers and researchers to investigate tornado related damage to RC structures.

References

- [1] LS-DYNA, Keyword User's Manual, Livermore Software Technology Corporation, CA (2015)
- [2] National Crash Analysis Center (NCAC), The George Washington University, USA
<http://www.ncac.gwu.edu/>
- [3] Malvar, L.J. et al.: A plasticity concrete material model for DYNA3D, *Int. J. of Impact Engineering*, Vol. 19, No. 9-10, pp. 847-873, 1997.
- [4] Madurapperuma, M., Niwa, K., Concrete material models in LS-DYNA for impact analysis of reinforced concrete structures, *Applied Mechanics and Materials*, Vol. 566, pp. 173-178, 2014.
- [5] Sugano, T. et al.: Local damage to reinforced concrete structures caused by impact of aircraft engine missiles part I: test program, method, and results, *Nuclear Engineering and Design*, Vol. 140, p. 387-405, 1993.
- [6] Sugano, T. et al.: Local damage to reinforced concrete structures caused by impact of aircraft engine missiles part II: Evaluation of test results, *Nuclear Engineering and Design*, Vol. 140, p. 407-423, 1993.